An Analysis of Wireless Signal Propagation in Collapsed Mine Scenarios

Asad Mahmood [1*], Muhammad Ahsan Ashraf [2,3], Godknow Musa [2,3,†] and Frederick Thomas Cawood [4]

[1] *Faculty of Engineering Sciences, Ghulam Ishaq Khan Institute of Engineering Sciences and Technology, Pakistan.*
[2] *School of Electrical and Information Engineering, University of the Witwatersrand, Johannesburg, South Africa.*
[3] *Sibanye-Stillwater Digital Mining Laboratory (DigiMine), University of Witwatersrand, Johannesburg, South Africa.*
[4] *Professor Emeritus, School of Mining Engineering, University of Witwatersrand, Johannesburg, South Africa.*

[*] *Corresponding author: asad.mahmood@giki.edu.pk*

† Deceased

Abstract

The missing miner problem arises when a miner working in an underground mine gets trapped after a mine collapse. The ability to precisely locate the missing miners is directly linked with the presence of a communications infrastructure that can allow communication with the trapped miners. The conventional communication systems commonly used in the mines, wired or wireless, are generally unable to communicate with the miners due to their limitations and damage because of the collapse. Wireless Sensor Networks may be more suitable in such scenarios; however, better understanding of the wireless signal propagation in collapsed mine scenarios can help in the design of robust systems which can provide connectivity even after the mine collapse. This paper analyzes the wireless channel in different scenarios related to a collapsed mine. The wireless channel is studied using simulations and real experiments in a mock mine. No such study exists to the best knowledge of the authors. Finally, suitable transmitted power levels that can be used in such scenarios are also determined.

Keywords: `collapsed mine, wireless sensor networks, wireless propagation channel, missing miner problem.`

1. Introduction

The mining industry is a significant contributor to the economy of most resource-rich countries. Although mining often starts as a surface operation, mines almost always require underground extension as the ore gets depleted in shallow areas. This, in turn, is making underground mines potentially hazardous working environments; hence, the news of partial or complete mine collapse is not so rare. For example, in a Chilean mine incident, a collapsed tunnel blocked the path, and 33 miners were trapped for 69 days. The rescue operation was impeded due to no communication with the miners [1].

The mine tunnels in underground mines sometimes experience rock fall, i.e., loose earth or inadequate roof support, which results in the partial or full collapse of the mine, such as in [2]. Sometimes miners get trapped as a result of the rock fall and a communications infrastructure is required for the tracking and rescue of the trapped miners.

The mine collapse almost always damages the existing communications infrastructure which jeopardizes the rescue operations. Such infrastructure is often attached to the roof or sidewalls of mine excavations. The existing communications infrastructure is commonly either a completely wired system, such as in [3], in which case the wires generally snap out, or it could be a hybrid system, e.g., a WiFi communication system that makes use of a fiber or LAN network backbone, in which case the wireless connectivity can break because of the inability of the WiFi signals to penetrate through the debris. There are through-the-earth (TTE) wireless communications systems that can penetrate earth/debris for large distances. However, these are large and bulky and hence cannot be carried by the miner, whereas a system closely accessible to the trapped miner is desired in the mine collapse scenarios. A Wireless Sensor Network (WSN) based system is more suitable for such scenarios, as mentioned in [4, 5, 6].

For such a WSN-based system, it is important to understand the channel

presented by a mine tunnel that has partially or fully collapsed. This will aid in designing a robust communication system, including the design of self-healing capabilities [7], which may be able to restore the communication link in case of a mine collapse. To the authors' best knowledge, no work exists in the literature that has studied the wireless channel for partially or/and fully collapsed mines in underground mine tunnels.

In this paper, we analyze the wireless channel in an underground mine tunnel in different mine collapse scenarios. A ray tracing-based analytical model [8] and the simulation tool of Altair WinProp [9] were used to estimate power loss profile in different mine collapse scenarios. Real-world experiments were also conducted in the *Wits mock-mine* [10], an underground mine tunnel built within the university premises replicating the tunnel of a real mine. This facility has been used previously to study the effect of tunnel structure on the channel for different antenna parameters [11], or for the design and testing of tracking devices for the rescue operation of the miners [7]. The result in this paper shows that signals power level degradation is a function of the height and width of the rock debris in the propagation medium. This information can be used to decide upon the transmit frequency and power levels which can be used to restore the communication link in case of a mine collapse.

Relevant literature review is discussed in section 2 of this paper, the methods are given in section 3, the simulation and experimental results and the associated discussions are presented in section 4, and finally the conclusion and future directions are given in section 5 of this paper.

2. Literature review

In order to achieve reliable and optimal performance of communication devices in high-stress underground mining environments, channel models for such environments need to be analyzed. A number of studies in literature have tried to characterize the communication channel for different underground mine and tunnels [12], [3], [13]-[14], although none of these tackle the case of a partially

or fully collapsed mine tunnel. For example, in [12], the channel model of the mine tunnel was studied by dividing the mine tunnel into three segments: (1) Line-of-sight (LOS), (2) Partial-line-of-sight (PLOS), and (3) Non-line-of-sight (NLOS), and fading profile of the channel was modeled using well-known Rician/Rayleigh fading distributions. The simulated and measured values were found to have good compromise in the characterization of the mine tunnel wireless channel. In another study, a higher path loss exponent was measured in the subway tunnel with a larger radius than in the tunnel with a smaller radius at 920 MHz, 2400 MHz, and 5705 MHz [3]. Similarly, in another study, it was observed that the path loss exponent was lower than that in the free space scenario, even in the case of the LOS situation, due to the additional reflections from the boundaries of the tunnel for an ultra-wideband channel in underground mines [13].

A novel model for tunnel LOS propagation was proposed to predict propagation losses in near and far regions with different characteristics [15]. The model was validated with measurements and utilized to investigate the impact of frequency, antenna position, and tunnel dimensions on the breakpoint location of the propagation regions by calculating propagation losses using a hybrid technique. The findings indicated that higher frequencies, corner antenna positions, and larger tunnel dimensions resulted in a break point of the propagation regions further away from the transmitting antenna. On the other hand, antenna gain had no impact on these breakpoint locations.

In [16], Rajan et al. analyzed radio signal behavior in different underground mines. They identified major factors contributing to significant propagation losses, outlined the impact of the depth of the underground mine on signal propagation characteristics, and discussed the role of mining methods on radio signal behavior. In [17], the authors proposed a multimode waveguide channel model through extensive experimental studies in an underground coal mine, which was found to be more accurate than the existing methods.

Zhang et al. presented a method incorporating surface roughness into the vector parabolic equation method used for electromagnetic (EM) wave propa-

gation modeling [18]. The proposed method was validated by comparing experimental data in various tunnel scenarios with the proposed model. Similarly, a new hybrid multimode waveguide model was proposed in [19], which combined roughness loss and tilt loss of walls to provide an analytical expression for received power at any position in a tunnel.

Branch et al. analyzed LoRa protocol [20] signal propagation in an underground block cave gold mine [21]. Block cave mining is an underground mining technique used to extract metals, usually gold, and copper, from hard rock, low-grade, and ore bodies. The results showed that LoRa performs well even in block cave mines and thus can be applied for different applications in underground mines.

Finally, in [14], a joint path loss model for radio propagation in cascaded straight and curved tunnels was proposed and verified through measurement and simulation results. The model combines waveguide mode theory and the method of shooting and bouncing rays to account for the extra loss introduced by the curvature of the tunnels and is shown to accurately predict path loss in cascaded tunnels with low complexity.

In a study by Hussain et al. [11], the impact of tunnel structure on channel modeling and antenna parameters was investigated for the Wits mock mine. It surveys different measurement campaigns and identifies open research areas. The potential of wireless sensor networks (WSN) for risk management in the mining industry, specifically in finding trapped miners in a disaster scenario, was explored [22]. A prototype sensor node was designed and tested at ISM bands to monitor miners' health and localize them. The sensor node outperformed traditional WSN nodes in disaster scenarios emulated inside the Wits mock mine. Similarly, in [23], a smartphone network for wireless communication in underground mining environments was investigated. The wireless system was tested for data transmission from sensors in various areas of Wits mock mine, achieving a communication speed of 80 Mbps over a 60m range, indicating potential for supporting applications with higher data rates.

A communication system that can effectively operate in disaster scenarios

is crucial for underground mines and tunnels. One such system is the proposed system in [24], which makes use of IEEE 802.15.6, NISA, and AODV protocols and was evaluated through simulations. Results indicated that high-priority nodes had less delay and energy consumption, while decreasing priority levels slightly increased delays and energy consumption.

3. Methodology

In order to study the channel for collapsed mine tunnel scenario, two scenarios were considered, i.e., (1) Partial collapse and (2) Full collapse. For the sake of simplification, in both scenarios, the mine tunnel was divided into 3 segments, as shown in Figure 1. In the partial collapse scenario, it was assumed that the fallen debris is only in segment 2, and the tunnel does not get fully blocked because of fallen debris, as shown in Figure 1a. In the full collapse scenario, however, it was assumed that the mine tunnel gets fully blocked because of the fallen debris, as shown in Figure 1b. The path loss profile was analyzed using three independent approaches where permissible; 1) Analytical approach using the ray-tracing method, 2) Computer-Aided Design (CAD) based simulations, and 3) Real-world experimentation. Details about these methods are given below.

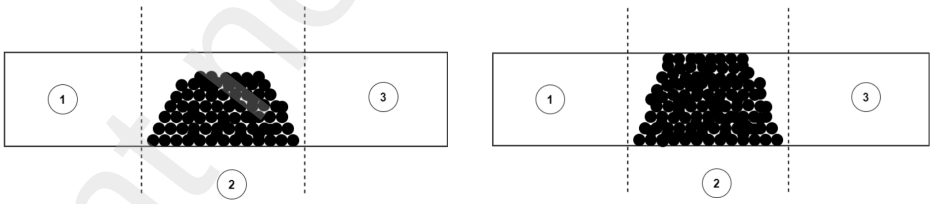

(a) Partial collapse scenario (b) Full collapse scenario

Figure 1: Segmentation of collapsed mine tunnel

3.1. Analytical Channel Modelling

For analytical modelling, the method proposed in [8] was utilized which is based on the use of the ray-tracing approach in tunnels. It uses a discrete number of rays to approximate high-frequency wave propagation. Each ray's power

decreases with distance, and its 3D path determines the distance traveled. Ray tracing involves following the ray path, where the ray travels in a straight line until they encounter surfaces that cause reflection, absorption, or diffraction. The process is repeated until a certain number of rays are transmitted. Ray tracing yields better results than other methods but is computationally expensive, with costs increasing as the number of receivers and surfaces increases. It is accurate for areas which are large relative to the wavelength [25]. In [26], the surface roughness was also included in the modelling. The overall attenuation which represents the average field attenuation at the receiver, is given as:

$$\bar{\alpha}(x,y,z) = \sum_{p=-\infty}^{\infty}\sum_{q=-\infty}^{\infty}\Big(\frac{\exp(-jkr_{p,q})}{r_{p,q}}\Big)(R_h^+S_h^+)^{|\frac{q+1}{2}|}(R_h^-S_h^-)^{|\frac{q}{2}|}(R_v^+S_v^+)^{|\frac{p+1}{2}|}(R_v^-S_v^-)^{|\frac{p}{2}|} \tag{1}$$

whereas, $\bar{\alpha}(x,y,z)$ represents average field attenuation at the receiver from all the propagation paths, $R_h^{\pm}$ represents ceiling and floor reflection coefficient, $R_v^{\pm}$ represents walls reflection coefficient, $S_v^{\pm}$ represents roughness coefficient for the vertical wall of the tunnel, $S_h^{\pm}$ represents roughness coefficient for the ceiling and floor of the tunnel (the signs differentiating between the two sides, e.g. left and right side wall), $r_{p,q}$ is the index of path taken by a ray, p is the number of reflections from the walls, and q is the number of reflections from the ceiling and floor.

Equation 1, which represents the attenuation, is then combined with the Friis equation through equation 2 to evaluate the received power in the various segments of the mine tunnel.

$$P(x,y,z) = P_t\Big(\frac{c}{4\pi f_0}\Big)^2|\bar{\alpha}(x,y,z)|^2 \tag{2}$$

whereas, c is the speed of light and P_t is transmitted power f_0 is the centre frequency of the signal.

The methodology used for channel modelling of the collapsed mine tunnel using the ray-tracing method of [8] is shown in Figure 2, where the tunnel is divided into three segments, with the fallen debris assumed to be only in segment 2, as

shown in Figure 1. Since the ray-tracing approach can only be used for the open segments of the tunnel, each segment of the tunnel was analyzed independently. The output power from segment 1 was considered as the input power to segment 2, and likewise, the output power of segment 2 was taken as the input power to segment 3. For segments 1 and 3, in which there is no collapse/debris, the ray tracing model [8] was used for modelling the wave propagation in both, partial and full collapsed mine tunnel scenarios. For segment 2 of the fully collapsed mine scenario, as shown in Figure 1b, a through-the-earth (TTE) [27] propagation model was employed.

A convenient expression of the relationship between the power received and the power transmitted is obtained by incorporating the Friis equation for segment 1, as follows:

$$\frac{P_r}{P_t} = G_r G_t \Big(\frac{\lambda}{4\pi R}\Big) e^{-2\alpha R} \tag{3}$$

where P_t represents power emitted from the transmitter, P_r represents the power at the end of segment 1, and G_t and G_r represents gain of transmitter and receiver, λ is the wavelength of the transmitted signal, R is the separation distance between transmitter and receiver and α is the attenuation constant of the medium.

For the segment 2 in the partial mine collapse scenario, a combination of Ray-tracing and TTE model were employed based on the height and the width of the fallen debris. Analytical modelling was done by implementing the representative mathematical models of the chosen TTA and TTE techniques using the MATLAB software.

3.2. CAD simulations

To compare and validate the analytical modeling, commercially available Altair WinProp software [28] was used, which is part of FEKO software suite [9]. Winprop was used to develop CAD model of the mine tunnel for different scenarios. The software allows to define arbitrary curves, cross sections and heterogeneous mine structures for a realistic representation of a mine tunnel.

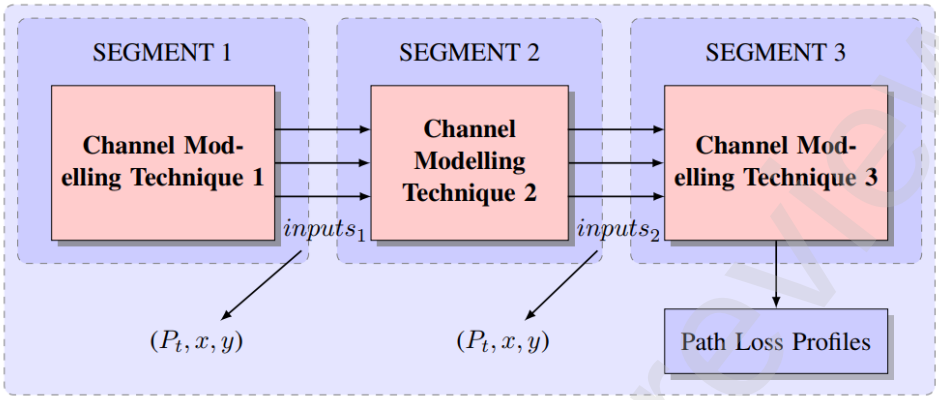

Figure 2: Schematic for channel modelling of collapsed mine tunnel

Different components of the software were used, such as *TuMan* defines the 3D structure of the tunnel, *WallMan* defines the electrical properties of the 3D structure of the tunnel, and *PropMan* carries the propagation simulations by specifying properties of antenna and placement. The simulations were performed for different frequencies and scenarios and results were recorded in form of 3D propagation heat maps and attenuation graphs. Different frequencies and transmit power levels were simulated using the Winprop software, and the corresponding results are given in the results section. The CAD model could only be employed for the non-collapsed mine tunnel scenario, as the feature to simulate the collapsed mine scenario was not available with the software. The procedure followed in 3D CAD simulation is shown in Figure 3.

3.3. Experimental setup

Real-world measurements were done using Zolertia RE-Mote based [29] nodes as the transmitter (Tx) and receiver (Rx) nodes, which are generally used for WSN prototyping, especially in the research space [30]. The nodes have a dual frequency capability via usage of an external mounted 915 MHz antenna and a surface-mounted 2.4 GHz antenna. A custom designed WSN node was used for testing 433 MHz. It consists of Atmega328P microcontroller and uses a RFM69 transceiver operating at 433MHz [22]. For the 2.4 GHz band, the nodes can

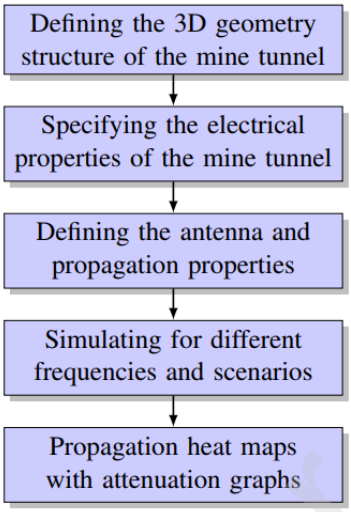

Figure 3: Procedure for 3D CAD simulation.

use a maximum transmission power of 3 dBm, and the nodes transmit at a maximum 14 dBm at 915 MHz. This is a limitation on the transmission power of nodes. For the 433 MHz band, the Atmega units can only make use of maximum transmission power of 7 dBm without the use of automatic transmission control, which will not allow to preset transmission power, but rather the node will have dynamic transmission power.

The test environment was an underground mock mine tunnel at the University of the Witwatersrand in the basement of the Chamber of Mines building [11, 31]. Same dimensions as that of the mock mine were used in the analytical modelling segment as well. Figure 4 shows the test setup with the nodes present inside the mock mine. The transmitting and receiving nodes were mounted at a height of 1.5 m using a tripod stand and in the middle of the tunnel.

RSSI (received signal strength indicator) was measured at the Rx node for different transmit power levels at the Tx node. The measurements were taken for different distances between Tx and Rx, in steps of 1 meter increase, over a total distance of 60 meters. Three independent measurements were noted for each case, and their average was considered for plotting. Serial communication was

established between a laptop and the Rx node to collect the RSSI values from the Rx node.

The measurements were conducted for the non-collapsed and the collapsed mine tunnel scenarios. The collapsed mine scenario was emulated by burying the transmitting node under a pile of sacks filled with sand, as shown in Figure 5b. Figure 5a shows the location of the transmitter node before the burial in a collapsed tunnel scenario.

Figure 4: Measurement setup in Wits Mock Mine

4. Results and Discussions

Simulated and measured results for the RSSI in different mine scenarios, via use of the different methods discussed in section 3.3, will be presented and discussed in this section.

4.1. Simulation Results

Simulated results for RSSI for different mine scenarios were generated using the analytical method and the CAD simulations method discussed the last

(a) Placement of transmitting node before burial

(b) Collapsed scenario with the transmitting node buried underneath the debris

Figure 5: Collapsed scenario for measurements setup in Wits Mock Mine

section 3. Simulation results were produced for different frequencies, especially the frequencies in ISM band suitable for WSN, or low frequencies which have better penetration properties.

4.1.1. No Collapse Scenario

In this scenario, no part of the mine tunnel was assumed to be collapsed. The attenuation constant at different points inside the mine tunnel was evaluated as per eq. 1 using parameters of the tunnel, as defined in Table 1. The electrical parameters used in the modeling represents the rock material found in underground mines. The results of path loss using the analytical method is shown in Figure 6, for different frequencies of interest. One can observe both the large-scale and the small-scale fading effects, which are due to constructive and destructive interference of the EM rays reflected from the mine tunnel boundaries. Interestingly, the average received power attenuates with a higher attenuation constant in the first half of the tunnel, as compared to the second half.

Table 1: Analytical modelling parameters of no collapse scenario

Parameter	**Values**	
Analytical tunnel dimensions	Height	3.0m
	Width	2.7m
	Length	90m
Electrical properties	Tunnel σ_r	0.015
	Tunnel ϵ_r	5
Antenna	Transmit power	1 mW
	G_t	1
	G_r	1
Modes	Total	100
	Smallest λ	0.059m
3D tunnel dimensions (for CAD simulations only)	Height	3.0m
	Width	2.7m
	Length	30m

In CAD simulations, the transmitter was placed at a height of 2 meters near the entrance point of the tunnel, and the receiver was moved at different points inside the tunnel, so as to vary the Tx-Rx distance, and keeping the same height. For the 3D CAD simulations, a total of 30 m tunnel length could only be simulated due to restrictions on the student license acquired. A rectangular tunnel was considered for the CAD simulations. The results for different frequencies of interest are shown in Figure 7. The bar in Figure 7 shows the rectangular tunnel with the Tx node placed at the bottom of the bar. The received power was mapped along the tunnel length for 30 m where each colour bar represents 1 m distance. The legends of Figure 7 represents the RSSI (dBm) values at different points in the tunnel. It can be seen that the received power decreases along the length of the tunnel. The used analytical model [8] and the CAD simulations are both primarily based on the ray tracing approaches with slight

modifications, such as the inclusion of surface roughness in [26], and the 3D ray tracing in the CAD simulations. Table 2 summarizes the results of both methods for 10 m, 20 m and 30 m length of the tunnel in no collapse scenario. It can be observed that the results have relatively good correlation for high frequencies whereas, there are large discrepancies at lower frequencies. This is because of the fact that the ray-tracing approach assumes the radio waves to behave as rays, which only happens when the wavelength of the propagating wave is smaller than the dimensions of the tunnel structure, i.e., only for large frequencies, as also discussed in another study [32].

Table 2: Comparison of Analytical and CAD results using ray tracing method where **A** represents Analytical results and **Sim** represent CAD simulation results for no collapse scenario

Frequency (MHz)	**RSSI values at different distances (dBm)**					
	10m		**20m**		**30m**	
	A	**Sim**	**A**	**Sim**	**A**	**Sim**
6.78	-30	-5	-36	-15	-40	-18
13.56	-34	-14	-39	-21	-40	-24
27.12	-37	-16	-43	-27	-42	-30
40.68	-40	-22	-42	-30	-46	-34
433	-48	-42	-58	-50	-56	-54
850	-52	-50	-60	-58	-63	-60
900	-53	-51	-64	-58	-58	-61
915	-52	-49	-64	-57	-60	-60
1800	-52	-55	-62	-63	-65	-65
2100	-54	-56	-58	-65	-64	-68
2300	-57	-58	-65	-66	-66	-68
2400	-57	-58	-60	-66	-68	-70
5800	-61	-64	-65	-73	-68	-76

Red represents difference of more than 10 dB, yellow represents difference of 4 dB - 10 dB and green represents difference of less than 3 dB.

4.1.2. Full Collapse Scenario

This section will present simulation results for the scenario where a segment of the mine has collapsed such that there are no air gaps in the collapsed segment, as shown in Figure 1b. The lengths of segment 1, 2 and 3 were taken as 30 m, 10 m, and 50 m, respectively.

WinProp's CAD simulation did not allow to simulate such a scenario in the software, and hence it was not used in this scenario. The method outlined in section 3.1 was used to simulate signal power degradation in this scenario, i.e., use of the ray-tracing based approach [8] for simulation of power loss in segment 1 and segment 3 of the mine as per Figure 1b, and use of a through-the-earth power loss modelling method [27] for simulating power loss in the collapsed segment (segment 2) of the mine tunnel.

The received power at the end of segment 1 was used as the input power for segment 2 and the received power at the end of segment 2 was considered as the input power for segment 3, as shown in Figure 2. In this scenario, the reflection coefficient was also taken into account when the wave enters from one segment/material to another. According to the electromagnetic theory, reflection coefficient describes the reflected power to the incident power from one medium to another medium. Equation 4 provides the reflection coefficient for the interface between layer i and the subsequent layer $(i+1)$ [33]:

$$\Gamma_{i,(i+1)} = \frac{\eta_{(i+1)} - \eta_i}{\eta_{(i+1)} + \eta_i} = -\Gamma_{(i+1),i} \tag{4}$$

$$\eta_i = \frac{j\omega\mu}{\gamma_i} \tag{5}$$

where, η_i represents the intrinsic impedance of the medium of wave propagation, ω is the angular frequency of the wave, μ is the permeability of the material, γ is a complex propagation constant, and j represents a complex number.

Equation 4 was used to determine transmitted power from segment 1 to segment 2 (air to rock) and from segment 2 to segment 3 (rock to air) of Figure 2. The sudden drops in the received power level at distances of 30 m and 40 m, as can be observed from Figure 8 represent the change of medium from air-to-rock and rock-to-air respectively. The interface between rock-to-air has a higher reflection coefficient than the air-to-rock interface, due to the higher permeability of rock compared to air. Therefore, the rock-to-air interface experiences greater reflection losses.

4.1.3. Partial collapse scenario

This section presents simulation results for the scenario where a segment of the mine has collapsed such that there are air gaps in the collapsed segment, as shown in Figure 1a. The lengths of segment 1, 2 and 3 were taken as 30 m, 10 m, and 50 m respectively, same as for the case for full collapse.

The Winprop's CAD simulation did not allow to simulate this scenario in the software, and hence CAD simulations were not used for this scenario as well. Signal degradation in segment 1 and segment 3 were modelled using the ray-tracing approach of [8] as was done for the 'full collapse' scenario, as there was no change in them. For segment 2, it was assumed that some part of the transmitted signal will pass through the air-gap on top of the fallen debris in segment 2, and this air-gap was approximately modelled as a tunnel of smaller dimensions.

A worst case partial collapse scenario for the height of the air-gap in segment 2, where a miner cannot crawl through and make it to the segment 3 from segment 1 through the middle collapsed segment. This minimum distance was considered to be 30 cm. It was assumed that a fraction of the rays will cross segment 2 through this gap after some reflections. Figure 9 shows the signal power degradation behavior in a tunnel with a smaller dimension of 30 cm. This behavior can be compared with the signal power degradation in a tunnel with larger height, as shown in Figure 6. It can be observed that the signal attenuation is much greater when the height of the tunnel is reduced to 30 cm. This is due to the fact that the signal has more reflections in the smaller tunnel compared to the tunnel with greater height.

4.2. Experiments based results

Real-world measurements were conducted inside the Wits mock mine using the setup and the scenarios mentioned in section 3.3. Figure 10a, 10b and 10c show the received powers for both, the no-collapse and full collapse scenarios, at 433 MHz, 915 MHz and 2.4 GHz, respectively. For the non-collapsed scenario, it can be observed that there is higher average degradation per unit distance

in the first half of the mine, and then the average degradation gets reduced/ flattened. This behaviour was also observed in the simulation results, as can be observed from Figure 6. The initial degradation in the signal power in the collapsed scenario was much higher than in the non-collapsed scenario, as was expected because the Tx node was buried under the sandbags for the collapsed mine scenario.

5. Conclusion

This study aims to analyze the wireless channel for underground mine scenarios when a portion of the mine has undergone a mine collapse. The study makes use of relevant analytical models, simulation tools and real-world experiments to analyse signal propagation in different collapse scenarios. To the best knowledge of the authors, no such study exists in the literature. It was observed that the attenuation increases drastically in the collapsed segment of the tunnel due to transmission losses at the interface of the rock and air which degrades the overall performance and coverage of the WSN in underground mine. The attenuation also increases with the increase in the frequency of the signal. This suggests usage of low-frequencies, however, a compromise would need to be made as very low frequencies result in large antennas which cannot be carried by the miner, and carrying of the WSN nodes by the miner can help in their traceability in case of a mine collapse.

Acknowledgement

The authors want to thank and acknowledge the financial support provided by the Sibanye-Stillwater Digital Mining Laboratory (DigiMine), Wits Mining Institute (WMI). This work is dedicated to the memory of Godknows Musa who contributed actively to the research leading to this paper. He was involved in the simulations and the experiments that led to the results presented in the paper.

Bibliography

[1] Eyewitness news: Lily mine collapses, last accessed 16 April 2023 (2016). URL `https://ewn.co.za/Topic/Lily-Mine-collapse`

[2] F. Rashid, A. C. Edmondson, H. B. Leonard, Leadership lessons from the chilean mine rescue., Harvard Business Review 91 (7-8) (2013) 113–9.

[3] K. Guan, B. Ai, Z. Zhong, C. F. López, L. Zhang, C. Briso-Rodríguez, A. Hrovat, B. Zhang, R. He, T. Tang, Measurements and analysis of large-scale fading characteristics in curved subway tunnels at 920 mhz, 2400 mhz, and 5705 mhz, IEEE Transactions on Intelligent Transportation Systems 16 (5) (2015) 2393–2405.

[4] L. Muduli, D. P. Mishra, P. K. Jana, Application of wireless sensor network for environmental monitoring in underground coal mines: A systematic review, Journal of Network and Computer Applications 106 (2018) 48–67.

[5] S. Sadeghi, N. Soltanmohammadlou, F. Nasirzadeh, Applications of wireless sensor networks to improve occupational safety and health in underground mines, Journal of safety research (2022).

[6] A. Chehri, R. Saadane, N. Hakem, H. Chaibi, Enhancing energy efficiency of wireless sensor network for mining industry applications, Procedia Computer Science 176 (2020) 261–270.

[7] I. Zaman, A. Förster, A. Mahmood, F. Cawood, Finding trapped miners with wireless sensor networks, in: 2018 5th International Conference on Information and Communication Technologies for Disaster Management (ICT-DM), IEEE, 2018, pp. 1–8.

[8] A. E. Forooshani, S. Bashir, D. G. Michelson, S. Noghanian, A survey of wireless communications and propagation modeling in underground mines, IEEE Communications surveys & tutorials 15 (4) (2013) 1524–1545.

[9] Altair, FEKO application, Altair Hyperworks, last accessed 16 April 2023.
URL https://www.altair.com/feko-applications/

[10] F. Cawood, Digital mine laboratory prepared for digital mining, last accessed 16 April 2023 (2015).
URL https://www.ee.co.za/wp-content/uploads/2015/03/positionit-march15-p26-30.pdf

[11] I. Hussain, F. Cawood, R. van Olst, Effect of tunnel geometry and antenna parameters on through-the-air communication systems in underground mines: Survey and open research areas, Physical Communication 23 (2017) 84–94.

[12] W. Farjow, K. Raahemifar, X. Fernando, Novel wireless channels characterization model for underground mines, Applied Mathematical Modelling 39 (19) (2015) 5997–6007.

[13] A. Chehri, P. Fortier, P. M. Tardif, Large-scale fading and time dispersion parameters of uwb channel in underground mines, International Journal of Antennas and Propagation 2008 (2008).

[14] J. Qian, Y. Wu, A. Saleem, G. Zheng, Path loss model for 3.5 ghz and 5.6 ghz bands in cascaded tunnel environments, Sensors 22 (12) (2022) 4524.

[15] Y. Zhang, Novel model for propagation loss prediction in tunnels, IEEE Trans. Veh. Technol. 52 (2003) 1308–1314.

[16] A. Ranjan, H. B. Sahu, P. Misra, Minesense: sensing the radio signal behavior in metal and non-metal underground mines, Wireless Networks 25 (2019) 3643–3655.

[17] A. Ranjan, H. Sahu, P. Misra, Modeling and measurements for wireless communication networks in underground mine environments, Measurement 149 (2020) 106980.

[18] X. Zhang, C. D. Sarris, Statistical modeling of electromagnetic wave propagation in tunnels with rough walls using the vector parabolic equation method, IEEE Transactions on Antennas and Propagation 67 (4) (2019) 2645–2654.

[19] X. Ji, C.-X. Wang, H. Chang, Characteristic analysis and modeling of underground space wireless communication channels, in: 2022 IEEE 95th Vehicular Technology Conference:(VTC2022-Spring), IEEE, 2022, pp. 1–5.

[20] J. Haxhibeqiri, E. De Poorter, I. Moerman, J. Hoebeke, A survey of lorawan for iot: From technology to application, Sensors 18 (11) (2018) 3995.

[21] P. Branch, Measurements and models of 915 mhz lora radio propagation in an underground gold mine, Sensors 22 (22) (2022) 8653.

[22] I. Zaman, A. Förster, A. Mahmood, F. Cawood, Finding trapped miners with wireless sensor networks, in: 2018 5th International Conference on Information and Communication Technologies for Disaster Management (ICT-DM), 2018, pp. 1–8. doi:10.1109/ICT-DM.2018.8636376.

[23] H. Ikeda, O. Kolade, M. A. Mahboob, F. T. Cawood, Y. Kawamura, Communication of sensor data in underground mining environments: an evaluation of wireless signal quality over distance, Mining 1 (2) (2021) 211–223.

[24] M. Cicioğlu, A. Çalhan, Performance analysis of ieee 802.15. 6 for underground disaster cases, Computer Standards & Interfaces 66 (2019) 103364.

[25] A. Emslie, R. Lagace, P. Strong, Theory of the propagation of uhf radio waves in coal mine tunnels, IEEE Transactions on antennas and propagation 23 (2) (1975) 192–205.

[26] C. Gentile, F. Valoit, N. Moayeri, A raytracing model for wireless propagation in tunnels with varying cross section, in: 2012 IEEE Global Communications Conference (GLOBECOM), IEEE, 2012, pp. 5027–5032.

[27] B. Austin, Radio communication in mines, Master's thesis, Thesis (M.Sc.(Eng))–University of the Witwatersrand, Faculty of Engineering (1977).
URL https://wiredspace.wits.ac.za/items/ced88705-d8b6-4b74-9ba1-77ad445a4099

[28] Altair, Radio coverage planning, last accessed 16 April 2023.
URL https://web.altair.com/winprop-telecom

[29] Re-mote revision a, last accessed 16 April 2023.
URL https://doc.riot-os.org/group__boards__remote-reva.html

[30] Zolertia, zolertia re-mote platform, last accessed 16 April 2023.
URL https://github.com/Zolertia/Resources

[31] M. A. Ashraf, A. Mahmood, M. A. Mahboob, Numerical evaluation of specific absorption rate in human head and torso for wearable wireless devices in underground mine scenarios, Radiation Protection Dosimetry 198 (8) (2022) 491–502.

[32] A. Hrovat, G. Kandus, T. Javornik, A survey of radio propagation modeling for tunnels, IEEE Communications Surveys & Tutorials 16 (2) (2013) 658–669.

[33] I. Dove, Analysis of radio propagation inside the human body for in-body localization purposes, Master's thesis, University of Twente (2014).

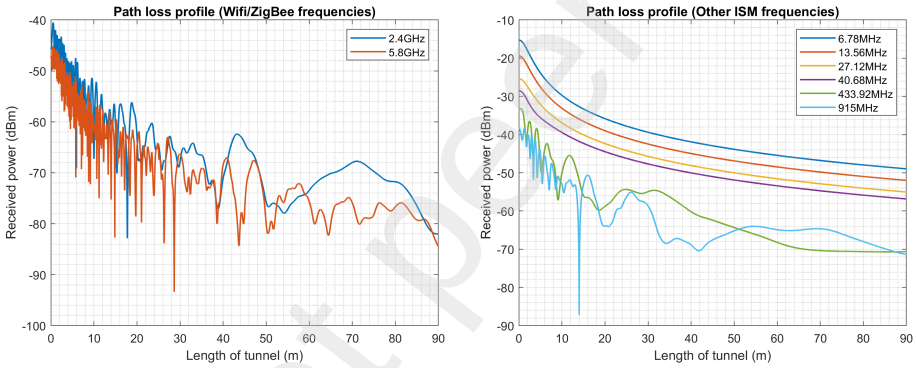

(a) (b)

Figure 6: Ray-optical tracing analytical modelling path loss profiles for no collapse scenario for (a) WiFi/ZigBee and (b) sub 1-GHz ISM frequencies.

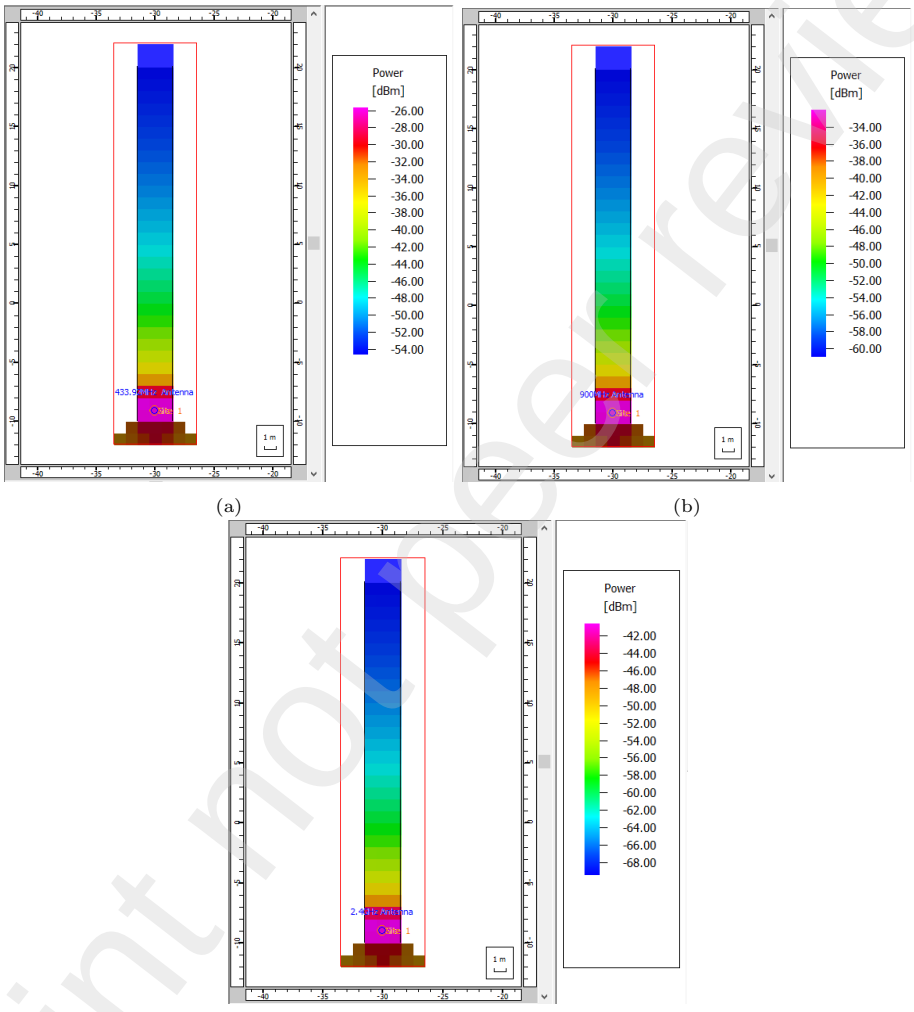

Figure 7: Tunnel 3D CAD propagation simulation received power heat maps for (a) 433 MHz, (b) 915 MHz, and (c) 2400 MHz.

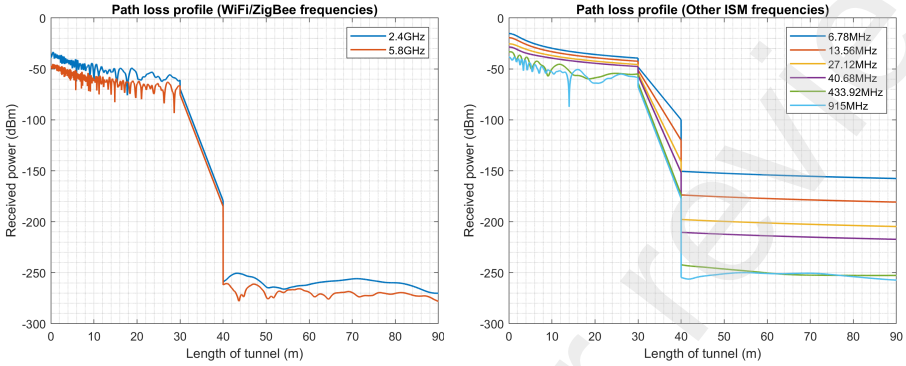

(a) (b)

Figure 8: Ray-optical tracing analytical modelling path loss profiles for full collapse scenario for (a) WiFi/ZigBee and (b) sub 1-GHz ISM frequencies.

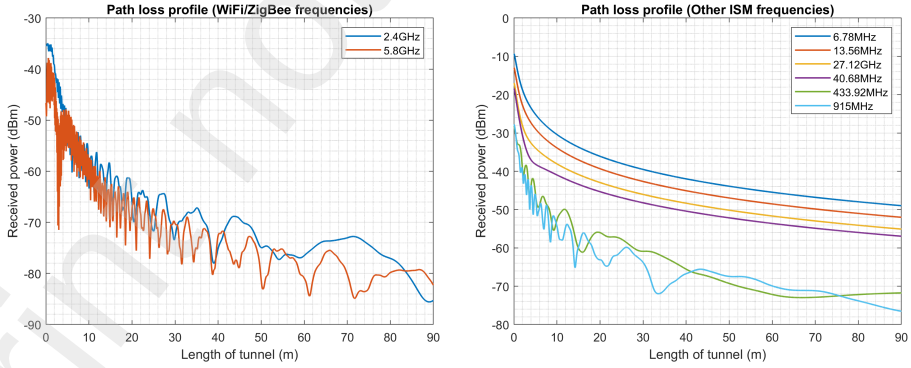

(a) (b)

Figure 9: Ray-optical tracing analytical modelling path loss profiles for partial collapse scenario for (a) WiFi/ZigBee and (b) sub 1-GHz ISM frequencies.

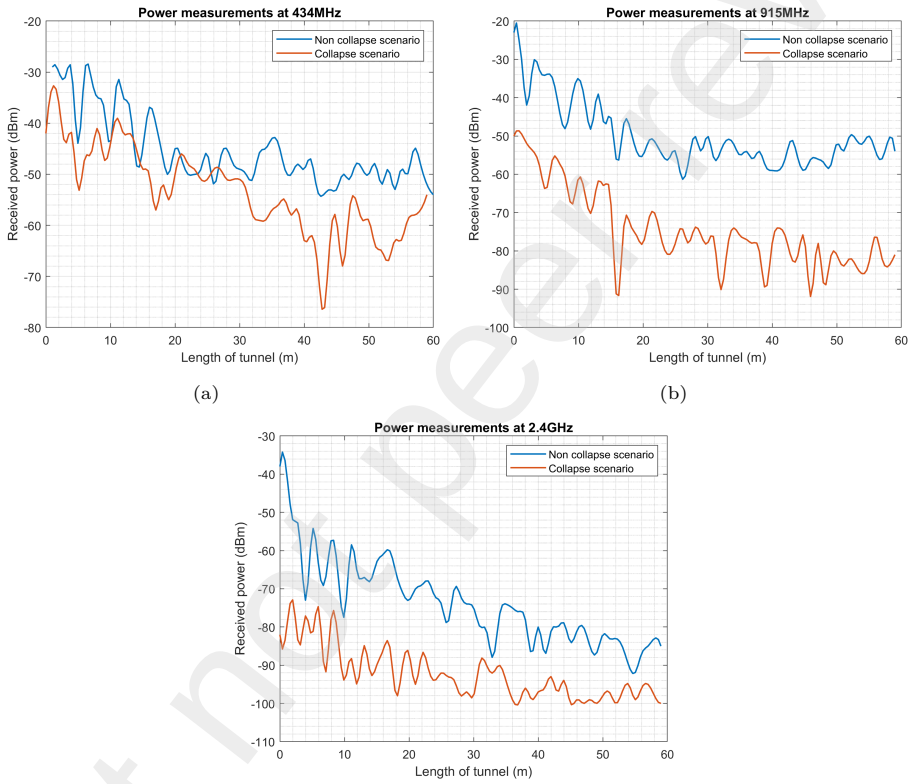

Figure 10: Comparison of results obtained for the collapsed and non-collapse scenarios at (a) 433 MHz, (b) 915 MHz, and (c) 2.4 GHz.